Design Optimization of a WIG Craft's High Lift Device Considering Ground Effect

Yiheng Wang[1,2], Wenping Song[1,2], Han Nie[1,2,], Kefeng Zheng[1,2], Zhonghua Han[1,2]

[1] Institute of Aerodynamic and Multidisciplinary Design Optimization, School of Aeronautics, Northwestern Polytechnical University, Xi'an, Shanxi 710072, People's Republic of China
[2] National Key Laboratory of Aircraft Configuration Design, Xi'an, Shanxi 710072, People's Republic of China

Abstract

The WIG (Wing-in-Ground) craft is a novel vehicle that makes use of the ground effect to realize cruising above the water. Contrary to the lift increase when a single wing in proximity of the ground at low angles of attack, the high lift device will experience a decrease in lift when in proximity of the ground, resulting in poor lift enhance when the high lift device is designed without considering ground effect, making it difficult to meet the takeoff requirements of low angles of attack, low speeds, and low flying heights for WIG crafts. In order to improve the lift increasing effect of the high lift device under low altitude conditions, this paper proposes a design optimization method for the high lift device of WIG crafts considering ground effect, which is based on a surrogate-based optimizer, a high lift device with significant lift increase was obtained at low altitudes. Firstly, based on the RANS solver, the aerodynamic performance of a two element high lift device designed without considering ground effect was evaluated. It was found that the high lift device would exhibit severe flow separation on the upper surface of the flap when in proximity of the ground, resulting in a significant reduction in lift of the high lift device. Therefore, it is not suitable for the WIG crafts that operate in the ground effect zone throughout the entire takeoff process. To address the above issues, with the abovementioned high lift device (designed without considering ground effect) as baseline, a design optimization for a high lift device considering ground effect is carried out, the results showed that the designed high lift device considering ground effect did not encounter flow separation when in proximity of the ground, resulting in a significant increase in takeoff lift by 26.6%. Further, targeting the high takeoff lift requirement of a certain WIG craft, taking the shape of flap's front slit, shape of flap's back slit, flap deflection angle and flap hinge position as design variables, an design optimization of the high lift device considering ground effect was carried out. The designed high lift device increased the takeoff lift by 34.7%. The WIG craft mounted with the designed high lift device resulted in an increase in takeoff lift from 10.3 tons to 11.1 tons tons, which makes an increase of 7.8%. The design optimization results verified the effectiveness of the method developed in this paper.

Keywords: Wing-in-Ground Craft, Ground Effect, Design Optimization, High Lift Device, Surrogate-based Optimization

1. Introduction

Ground effect refers to the phenomenon that the flow beneath the aircraft is compressed due to the influence of the wall, resulting in greater lift when the aircraft is flying at low altitudes [1][2]. The WIG (Wing-in-Ground) craft is a novel high-speed transport platform that achieves low-altitude flight by utilizing the ground effect [3], by taking full advantage of ground effect, the WIG craft makes lift-drag ratio increased and aerodynamic efficiency greatly improved [4]. Therefore, the development of WIG has a wide range of prospects, which includes transportation, travelling and rescue purpose [5]. By combining the characteristics of ships and aircrafts, WIG crafts possess the abilities of takeoff and landing on water as well as low-altitude flight. Compared to ships, WIG crafts have higher cruising speed; compared to seaplanes, WIG crafts have higher lift-to-drag ratios by taking advantage of ground effect. However, unlike a single wing, the high lift device doesn't increase lift when close to the ground, but rather has lift reduction [6][7], which is not conducive to the low-altitude takeoff of WIG craft. The takeoff and landing performance of an aircraft is a key indicator that must be considered in aircraft design [8]. High lift devices with good aerodynamic performance can effectively improve both the performance and safety of aircraft during takeoff phases [9][10]. In the past few decades, there has been a significant amount of research on the design of high lift device shapes. J Luo et al. proposed a new design method for

the adaptive dropped hinge flap (ADHF), through the design of flap shape, flap deflection angle, hinge position and length of spoiler chord, the takeoff lift-to-drag ratio of optimized flap was increased by 11.87% [11]. Zhou W Y et al. selected flap hinge position, flap deflection angle, and spoiler deflection angle as design objectives to carry out multi-objective aerodynamic optimization design for takeoff, landing and cruise conditions. The result showed that the optimized flap increased takeoff lift by 2.78%, landing lift by 6.27%, and the lift-to-drag ratio in cruise state improved by 17.9% [12]. JI Q et al. conducted a design optimization of the flap shape based on the 30P30N airfoil, with high takeoff lift as the target. By the design of the leading-edge flap position, trailing-edge flap position and spoiler position, the takeoff lift of optimized flap was increased by approximately 11.87% [13]. Tyan M et al. carried out design optimizations for both the airfoil and flap successively, by performing flap shape design on the optimized airfoil, the takeoff lift of optimized flap was increased by 9.87% [14]. Conventional aircraft has a larger takeoff climb angle during takeoff to quickly exit the ground effect zone. Existing high lift device design methods and empirical formulas do not consider the influence of the ground, resulting in a significant decrease in high lift devices designed based on these methods in proximity of the ground, rendering them unsuitable for WIG crafts. To solve this problem, this paper proposes a design optimization of a WIG craft's high lift device considering ground effect. By considering the influence of the ground effect, the high lift device designed by this method that can maintain high lift when in proximity of the ground, thus significantly increasing the takeoff lift of WIG crafts. In the second section, the numerical computational methods and aerodynamic design optimization methods used in this paper are outlined.In the third section, an aerodynamic performance of a high lift device is conducted by the RANS equation solver. It is observed that severe flow separation occurs at the trailing edge of the flap when in proximity of the ground, leading to a significant lift reduction. Subsequently, based on this high lift device, a design optimization of high lift device considering ground effect is carried out, resulting in improved aerodynamic performance at low-altitude flight. In the fourth section, a certain WIG craft is selected as an example to conduct a high lift device design optimization considering ground effect for higher takeoff lift. By using global surrogate-based optimization, the designed high lift device greatly improves the takeoff lift of the WIG craft.

2. Methodology

2.1 CFD Method and Validation

2.1.1 CFD Method

In this paper, the governing flow equations solved are the Reynolds-Averaged Navier-Stokes (RANS) equations with the Spalart-Allmaras turbulence model, which is expressed as:

$$\nabla \cdot \vec{V} = 0 \tag{1}$$

$$\rho \frac{\partial \vec{V}}{\partial t} + \rho \vec{V} \cdot \nabla \vec{V} = -\nabla \vec{p} + \nabla \vec{\tau} + \rho \vec{g} + \vec{S}\rho \tag{2}$$

The temporal discretization uses the implicit LU-SGS scheme, and the spatial discretization adopts the Roe upwind scheme with a minmod limiter.

2.1.2 Validation

In order to verify the numerical simulation capability of the numerical model for considering the ground effect, a NACA0012 wing model flying near the wall is chosen as a case for validation. Figure 1 shows the geometric model used in the wind tunnel test. Yang M, Jia Q et al. conducted a wind tunnel test on the ground effect wing model and published some experimental data [15] [16] [17]. The chord length of the wing is 400mm, the aspect ratio is 2.5, and the relative flight height h/c=0.1 (the height above the ground at the trailing edge). The Reynolds number of the test is $Re=1.4\times10^6$, the velocity of wind in the wind tunnel is 50m/s, and the moving belt speed is the same as the wind speed.

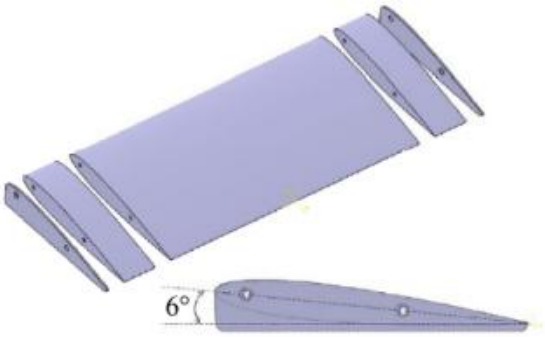

Figure 1 Wing model of wind tunnel test [15]

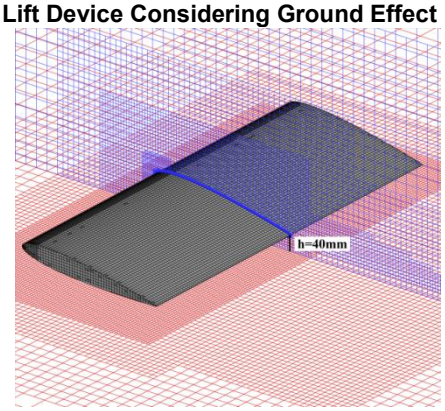

Figure 2 Diagram of mesh

Figure 2 shows the mesh, which uses a body-conforming Cartesian mesh and a prism layer mesh. The height of the first layer grid is 7.0×10-6m, and the growth ratio of the prism layer mesh is 1.2. The far field radius is about 100 times the chord length of the wing. The mesh is refined for the wing leading edge and the space below the wing. The number of mesh is approximately 1.5 million.

Figure 3 shows the comparison of the numerical simulation results with wind tunnel test results. The calculated value of lift closely matches the experimental value, and although there are some differences between the calculated and experimental values of drag, the deviations are small and the overall trend remains consistent. Overall, the calculated and experimental results show good agreement, demonstrating the accuracy and reliability of the numerical method used in this paper for ground effect problems.

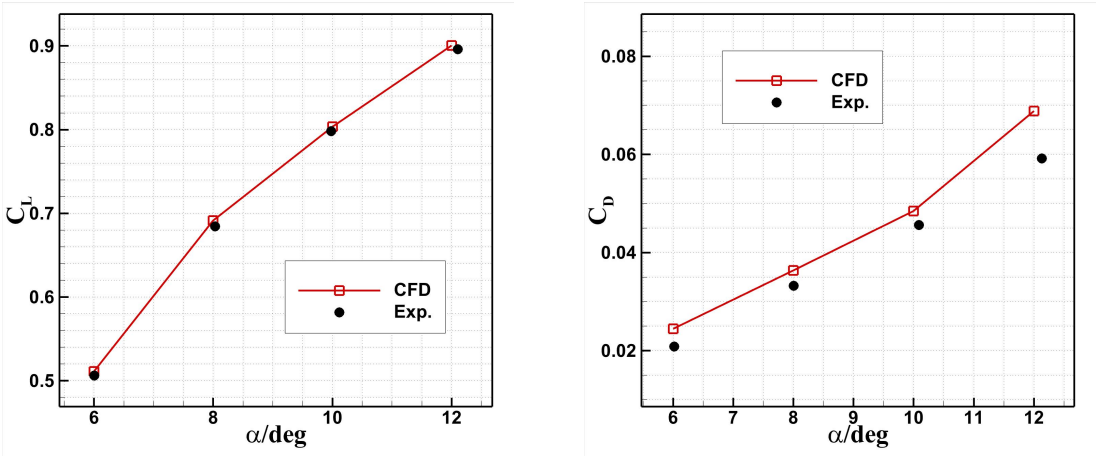

(a) Lift - angle of attack (b) Drag - angle of attack

Figure 3 Comparison of numerical simulation results with wind tunnel test values

2.2 Efficient Global Surrogate-based Optimization Method

The surrogate-based optimization method has received extensive attention in the aerospace and other fields due to its ability, and has gradually developed into a class of optimization algorithms called surrogate-based optimization (SBO) algorithms. In recent years, Professor Han's group at Northwestern Polytechnical University has made a series of research progress in the theory and application of surrogate-based optimization algorithms, and has developed a proprietary general surrogate-based optimization toolkit called "SurroOpt" [18]. In this paper, a global surrogate-based optimization method is used in the design optimization of high lift device. A description of the surrogate-based optimization process is shown in Figure 4.

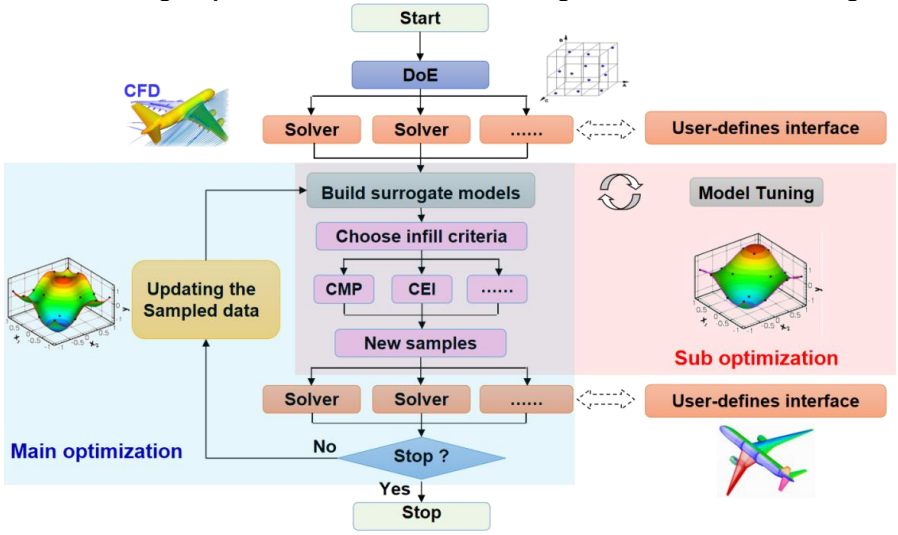

Figure 4 Flow chart of the global surrogate-based optimization method [19]

2.3 Parameterization Method

The CST parameterization method (Class function/Shape function Transformation) is a parameterization method for describing the two-dimensional geometric shape based on shape function/class function transformation, proposed by engineer Kulfan of Boeing Company in 2008 [20]. Due to its advantages of ensuring high fitting accuracy while avoiding the occurrence of wave-like shapes, the CST parametric method is used in this section for parametric processing of the flap shape. The CST parameterization method consists of a class function $C(x)$ and a type function $S(x)$, as expressed follow:

$$y = C(x) \cdot S(x) \tag{3}$$

Where the class function $C(x)$ and type function $S(x)$ are:

$$C(x) = x^{N1} \cdot (1-x)^{N2} \tag{4}$$

$$S(x) = \sum_{i=0}^{N} A_i \cdot S_i(x) \tag{5}$$

$N_1 = 1$, $N_2 = 1$,and using Bernstein Polynomial to construct function: $S_i(x)$:

$$S_i(x) = \frac{N!}{i!(N-i)!} x^i (1-x)^{N-i} \tag{6}$$

Where N is the order of the polynomial and i is the exponent of the polynomial. In this paper, 8th-order CST parameterization is used to parameterize flap shape. Figure 5 shows the polynomial curve of the 8th-order CST parameterization method. The fitting and control of flap contour can be realized by weighted superposition of each curve in the figure. A_i is the weight coefficient of the curve, and the change of the value A_i can be completed to change the flap shape.

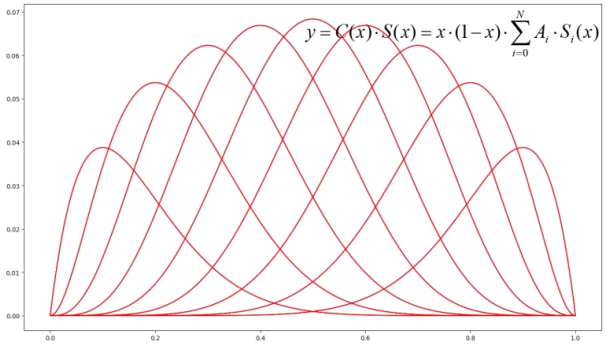

Figure 5 8th-order CST parameterization method

3. Comparison of Takeoff Aerodynamic Performance of High Lift Devices

3.1 High Lift Device without considering Ground Effect

The aerodynamic performance of the high lift device without considering ground effect and at flight altitude of one chord is conducted. The geometric shape of the high lift device is shown as Figure 6. Table 1 provides the calculation settings. Figure 7 shows the mesh without ground boundary, with free flow boundary conditions. The far field radius is about 100 times the chord length, and the height of the first layer mesh is 1.1×10^{-5}m. The total number of mesh is about 130 thousands. Figure 8 shows the mesh at flight altitude of one chord at the leading edge. To simulate the ground, the boundary below the high lift device uses the wall boundary condition. The total number of mesh is approximately 110 thousands.

Table 1 Takeoff state calculation parameter

Calculation setting	Value
Temperature (K)	288.15
Density (kg/m^3)	1.225
Velocity (m/s)	36
Chord (m)	3.5
Angle of attack (deg)	8.3
Reynolds number	2.4×10^6

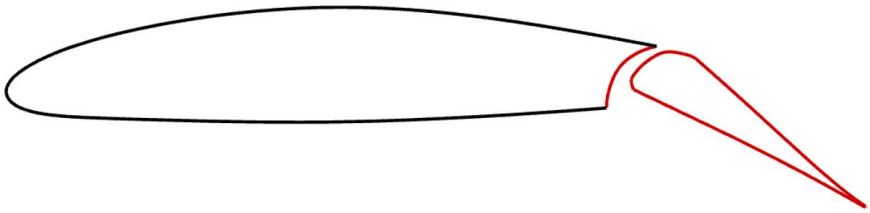

Figure 6 High lift device without considering ground effect

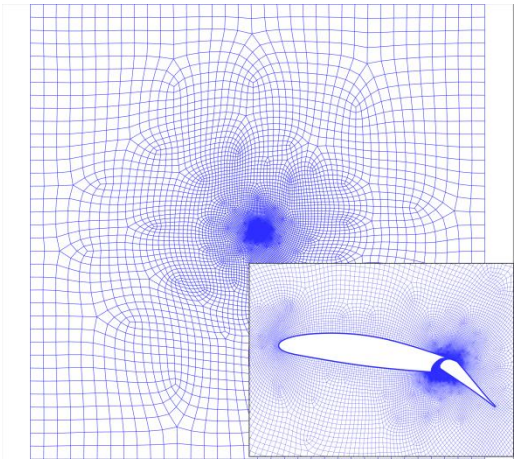

Figure 7 mesh without ground boundary

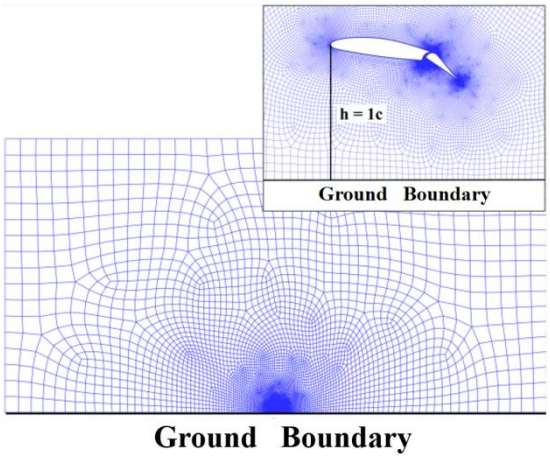

Figure 8 mesh of a flight altitude of one chord

The numerical simulation results of the high lift device without ground effect and at flight altitude of one chord are shown in Table 2 and Figure 8. From Table 2 we can see that compared with the condition without ground effect, the aerodynamic performance of the high lift device is significantly reduced at flight altitude of one chord, with not only a decrease in lift coefficient from 2.5400 to 1.7996, a reduction of about 29%, but also an increase in drag by about 26.8%. From the flow field in Figure 9, it can be seen that severe flow separation occurs behind the flap when the Figure 9 is close to the ground, which is the main reason for the significant reduction in aerodynamic performance.

Table 2 Aerodynamic comparison of the high lift device

Condition	C_l	ΔC_l	C_d	ΔC_d
No ground effect	2.5400	—	0.0512	—
Flight altitude of 1c	1.7996	**↓29.1%**	0.0649	**↑26.8%**

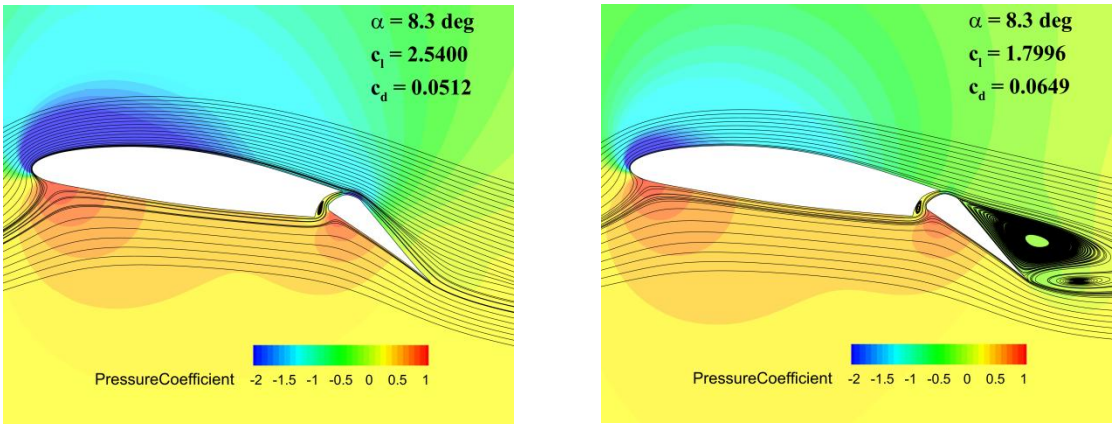

(a) No ground effect (b) Flight altitude of 1c

Figure 9 Comparison of the high lift device's flow field

3.2 Design Optimization of High Lift Device Considering Ground Effect

The design optimization method for high lift device tends to have a significant reduction in lift effectiveness when approaching the ground. This paper proposes a design optimization method for high lift device considering ground effect. Based on the high lift device design in Section 3.1, the design optimization of high lift device considering ground effect is conducted.

The design variables are: shape of flap's front slit (8th order CST method), shape of flap's back slit (8th order CST method) and flap's position (movement in the x axis and y axis), and there are 18 design variables. The lift coefficient is selected as the objective function for design optimization, and the optimization problem is defined as follows:

$$\min. \quad -c_l \tag{7}$$

Figure 10 presents a geometry comparison between the designed high lift device considering ground effect and the baseline from Section 3.1, and the aerodynamic performance of both devices is evaluated with reference to Table 1, Figure 7 and Figure 8.

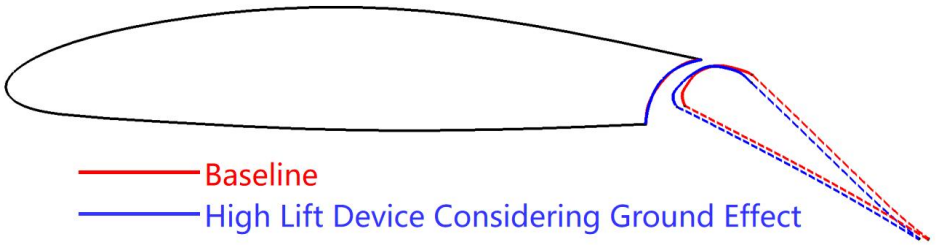

Figure 10 Geometry comparison of high lift devices

The aerodynamic performance evaluation is shown in Table 3 and Figure 11. It can be seen that the lift of high lift device designed considering ground effect has a slight reduction when the flight condition is no ground effect, decreasing the lift by 4.26% compared to the baseline. However, the takeoff lift at height of one chord is much greater than the baseline, with a lift coefficient increasing from 1.7996 to 2.2779, an increase of 26.6%. By comparing the flow field information in Figure 11, we can see that the high lift device designed considering ground effect can still maintain attached flow on the upper surface of the flap at little flight altitude, therefore it can maintain high lift.

Table 3 Aerodynamic comparison of two high lift devices

High lift device	Condition	C_l	ΔC_l
Baseline	No ground effect	2.5400	—
High Lift Device Considering Ground Effect		2.4316	↓**4.26%**
Baseline	Flight altitude of 1c	1.7996	—
High Lift Device Considering Ground Effect		2.2779	↑**26.6%**

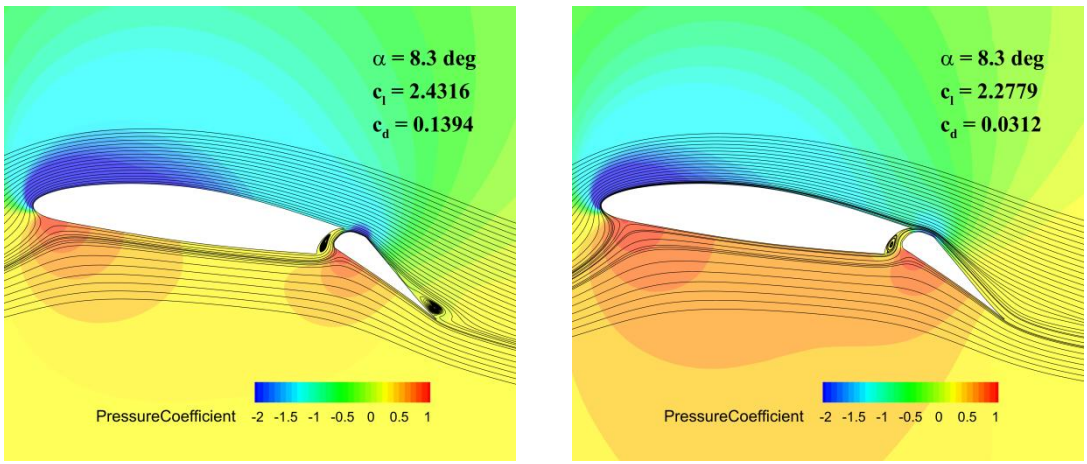

(a) No ground effect (b) Flight altitude of 1c

Figure 11 Comparison of designed high lift device's flow field

From the above, we can see that design methods, due to not considering the influence of ground effect, result in a significant lift reduction of high lift device when the close to the ground. So these high lift devices designed by conventional design methods are not suitable for the WIG craft that works in the ground effect zone for a long period of time. Therefore, when designing high lift device for WIG crafts, it is crucial to consider the influence of ground effect.

4. Design Optimization Considering Ground Effect for a WIG Craft's High Lift Device

Based on the design optimization method of high lift device considering ground effect from previous section, this section carries out a design optimization considering ground effect for a WIG craft's high lift device. The design variables are: flap's front slit (8th order CST method), shape of flap's back slit (8th order CST method), flap deflection angle and flap hinge position (x position and y position), and there are 19 design variables. Figure 12 shows the baseline shape. A Latin hypercube sampling method is used to generate 40 initial sample points, including the baseline, which are used to establish an initial surrogate model [21]. MSP+EI parallel point addition methods [22][23] are selected as the adding point strategy. The lift coefficient is selected as the objective function for design optimization, and the optimization problem is defined as follows:

$$\min. \quad -c_l \tag{8}$$

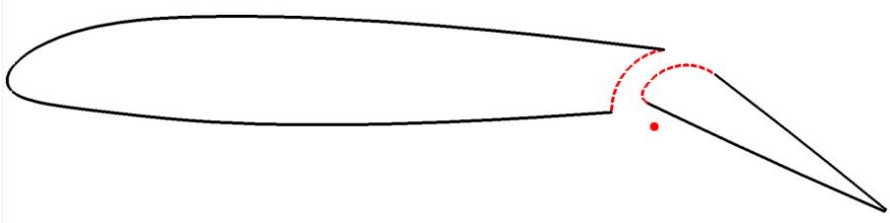

Figure 12 Baseline shape

In order to prevent the waves from hitting the lower part of the flap during the takeoff sliding phase of WIG crafts, it is necessary to restrain the position of the flap. Figure 13 shows the position constraint of the flap, with the lowest point of the flap required to be higher than the baseline. To

meet this requirement, limitations on the flap hinge position and the deflection angle of the flap are specified in Table 4.

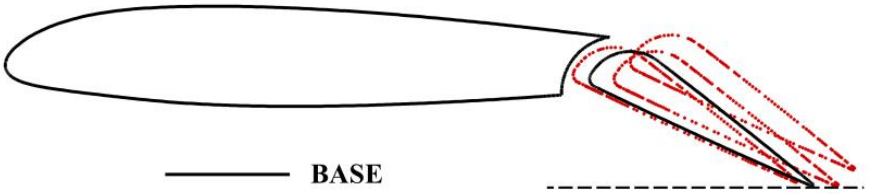

Figure 12 Position constraint of the flap

Table 4 The upper and lower bounds of the hinge position and deflection angle

Upper and lower bounds	x position of hinge	y position of hinge	Deflection angle δ_f (deg)
Lower bound	0.7 c	-0.08 c	25
Upper bound	0.8 c	-0.03 c	30

Figure 14 presents the mesh used in the design optimization, which utilizes a automatically generated unstructured mesh. The height of the first layer mesh is 1.1×10^{-5}m, and the far field radius is about 100 times the chord length, with a total mesh volume of about 130 thousands. To simulate the ground, a wall boundary condition is applied to the bottom boundary of the mesh. The calculation settings are given in Table 5.

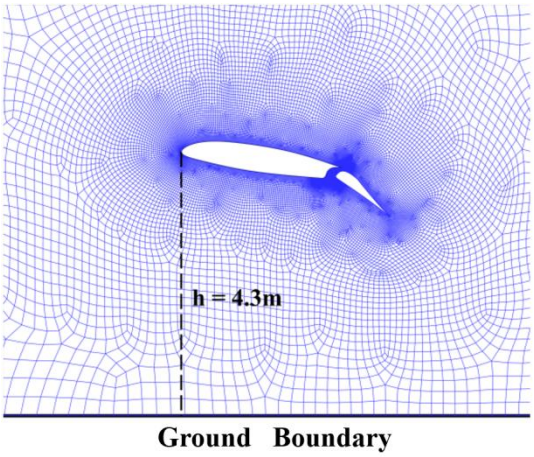

Figure 14 Mesh of high lift device

Table 5 Takeoff state calculation parameter setting

Calculation Setting	Value
Temperature (K)	288.15
Density (kg/m^3)	1.225
Velocity (m/s)	36
Flight altitude (m)	4.3
Chord (m)	3.5
Angle of attack (deg)	9.8

Figure 15 shows the convergence process of the design optimization, and Figure 16 compares the shape of the designed high lift device and baseline. The flap hinge position of the designed high lift device is lower, resulting in a slight increase in the chord length of the "deflected airfoil". Regarding the deflection angle of the flap, it is optimized to an upper bound of 30°.

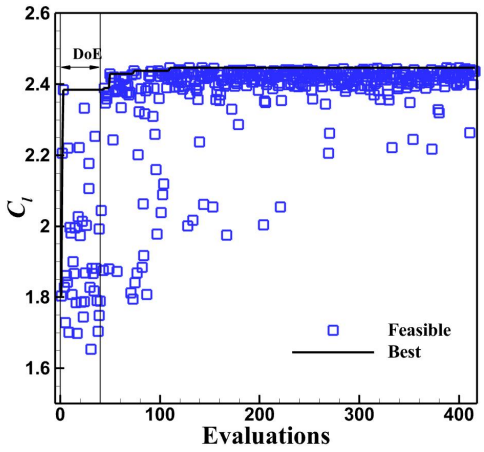

Figure 15 Convergence process

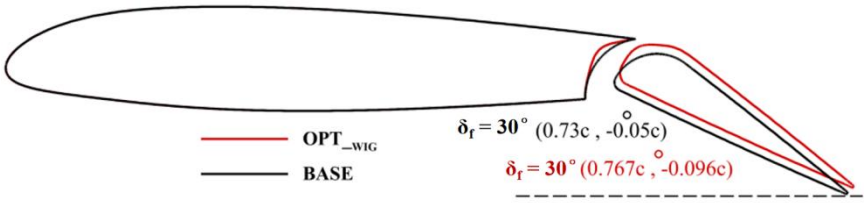

Figure 16 Shape comparison of the designed high lift device and baseline

The aerodynamic performance of the baseline and the designed high lift device considering ground effect are compared by referring to the calculation state in Table 5. The numerical simulation results are shown in Table 6 and Figure 17. It can be seen that compared with the baseline, the designed high lift device improves the flow behind the flap, and solves the problem of flow separation. Therefore the aerodynamic characteristic has a great improvement, the takeoff lift coefficient is increased from 1.8126 to 2.4493, an increase of about 34.7%, and the lift-drag ratio is also increased by 212%.

Table 6 Aerodynamic comparison of two high lift devices

High lift device	C_l	ΔC_l	C_l/C_d	$\Delta C_l/C_d$
Baseline	1.8186	—	26.98	—
Designed High Lift Device	2.4493	**↑34.7%**	84.16	**↑212%**

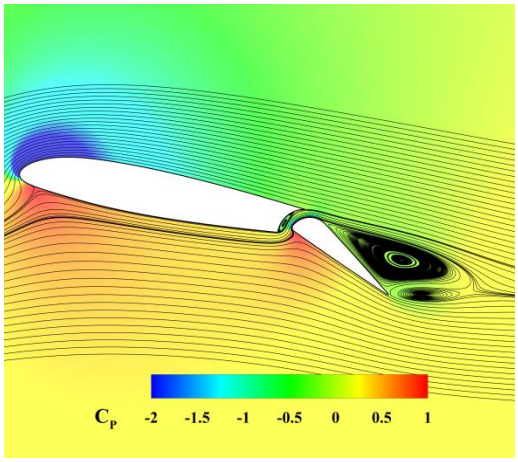

(a) Baseline

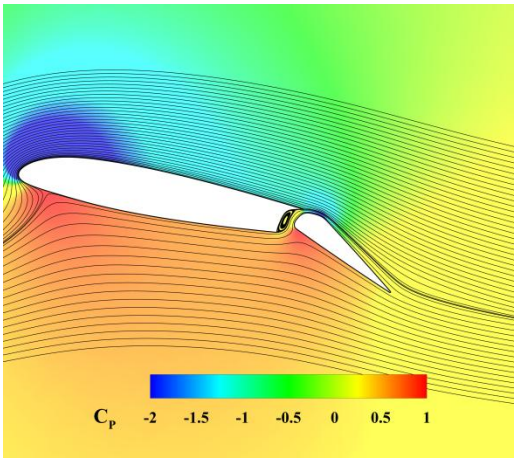

(b) Designed high lift device

Figure 17 Comparison of baseline and designed high lift device's flow field

Subsequently, a takeoff aerodynamic performance comparison is conducted for the WIG craft mounted with the baseline and designed high lift devices. Table 7 provides the takeoff state of the WIG craft, and Figure 18 shows the mesh of a WIG craft. The height of the first layer mesh is 1.2×10^{-5}m, and the total mesh volume is about 45 million.

Table 7 Takeoff state of the WIG craft

Calculation Setting	Value
Temperature (K)	288.15
Density (kg/m^3)	1.225
Velocity (m/s)	36
Flight altitude (m)	0.1
Average chord (m)	3.5
Angle of attack (deg)	6
Gravitational acceleration (m/s^2)	10

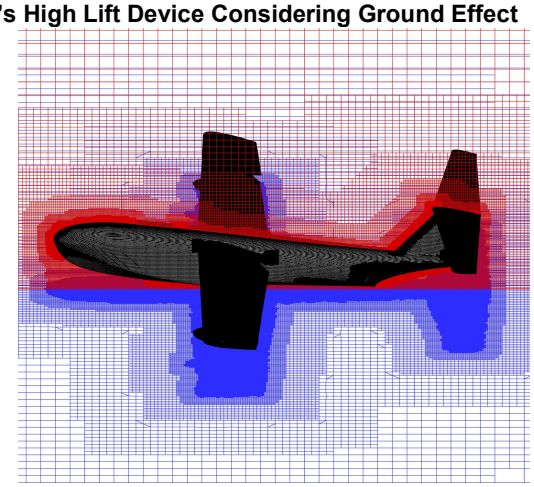

Figure 18 Mesh of WIG craft

Table 8 provides a comparison of the takeoff aerodynamic performance between the baseline takeoff configuration (using baseline high lift device) and the designed takeoff configuration (using designed high lift device). Compared to the baseline, the designed high lift device can still provide better lift enhancement on the WIG craft. The takeoff aerodynamic performance the designed takeoff configuration mounted with the designed high lift device has significantly improved compared to the baseline takeoff configuration, with a lift increase from 10.3 tons to 11.1 tons, representing an improvement of about 7.9%. The lift-to-drag ratio has also increased by approximately 11.8%.

Table 8 Comparison of aerodynamic performance between the baseline and designed take-off configuration

Configuration	Lift (N)	ΔLift	C_l	C_l/C_d	$\Delta C_l/C_d$
Baseline takeoff configuration	103184	—	2.0278	13.05	—
Designed takeoff configuration	111326	↑**7.8%**	2.1878	14.59	↑**11.8%**

Fig. 19 presents a comparison of the flow fields between the baseline takeoff configuration and the baseline takeoff configuration. Similar to the flow of a 2D high lift device, the baseline takeoff configuration with baseline high lift device also experiences severe flow separation on the upper surface of the flaps, resulting in poor lift enhancement. On the other hand, the designed takeoff configuration maintains a large area of attached flow on the upper surface of the flaps, with only a small amount of flow separation in small regions. Therefore, the takeoff aerodynamic performance has been significantly improved.

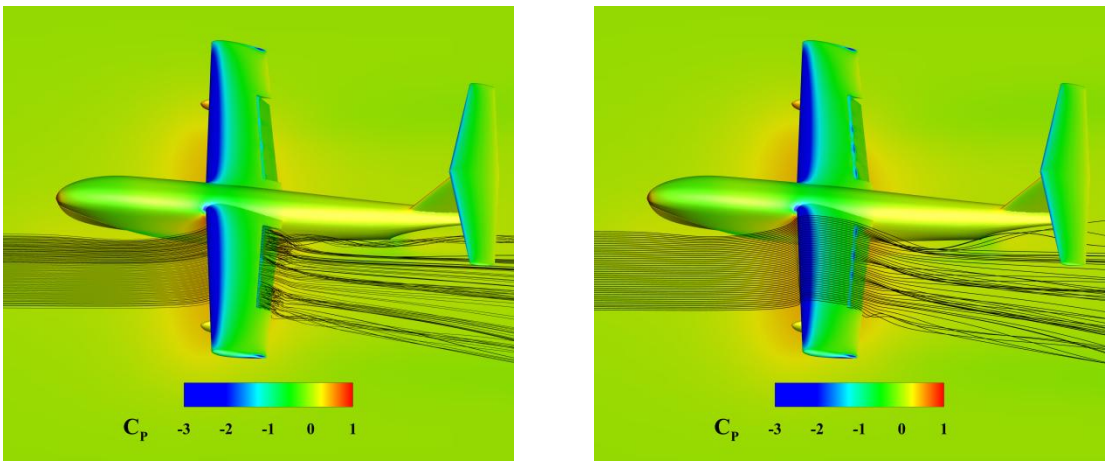

(a) Baseline takeoff configuration (b) Designed takeoff configuration

Figure 19 Comparison of takeoff configuration's flow field

5. Conclusions

This paper proposes a design optimization method considering ground effect for a WIG craft's high lift device and carries out a design optimization of a high lift device for high-lift aerodynamic performance.

(1)High lift device design methods, due to not considering the influence of ground effect, result in a significant decrease when in proximity of the ground, which is not suitable for the WIG crafts that operate in the ground effect area for prolonged periods. For WIG crafts, when designing high lift device, it is crucial to consider the influence of ground effect.

(2)Aiming at the problem that the lift of high lift device is weakened when in proximity of the ground, this paper proposes a design optimization method considering ground effect for a WIG craft's high lift device and selects a certain WIG craft as an example to conduct high-lift design optimization for higher takeoff lift. By optimizing the high lift device considering the ground effect, the takeoff lift of the WIG craft mounted with the designed high lift device increases from 10.3 tons to 11.1 tons, representing an improvement of about 7.8%, and the lift-to-drag ratio also increases by about 11.8%, which significantly enhances the takeoff aerodynamic performance.

6. Acknowledgment

The calculations were performed on Sugon.

7. Contact Author Email Address

Wenping Song *, wpsong@nwpu.edu.cn, corresponding author.

8. Copyright Statement

References

[1] Wiriadidjaja S, Mohamad Z H, Rafie A S M, et al.Wing-In-Ground-Effect Craft as a Potential Domestic Transport Vehicle[C]. Aiaa Applied Aerodynamics Conference. 2015.

[2] Rozhdestvensky K V. Aerodynamics of a Lifting System in Extreme Ground Effect[M]. Berlin: Springer, 2000.

[3] Halloran M, O' Meara S, Wing in Ground Effect Craft Review[R]. Dsto-Gd-0201, 1999.

[4] Shi Y J, Ma D P, Zhao H F, et al. Research on The Safety Operation Limits of the WIG [M]. France: Fast Sea Transportation Innovative Materials, 2017: 301-308.

[5] Volkov L.D, Ponomarev A.V, Treschevski V,N, Yushin V.I, 1992, Results of Aerodynamic Research Carried out in Krylov Institute in Support of Design of Ekranoplans. International Proceedings of the Second International Conference on High Speed Ships.

[6] Qu Q L, Wang W, Liu P Q, et al. Aerodynamics and Flow Mechanics of a Two-Element Airfoil in Ground Effect[C]. 53rd Aiaa Aerospace Sciences Meeting, Jan. 2015.

[7] Qu Q L, Ju B B, Huang L W, et al. Flow Physics of a Multi-Element Airfoil in Ground Effect[C]. 54th Aiaa Aerospace Sciences Meeting, Jan. 2016.

[8] Van Dam C P. The Aerodynamic Design of Multi-Element High-Lift Systems for Transport Airplanes[J]. Progress In Aerospace Sciences, 2002, 38(2): 101-144.

[9] D. Reckzeh, Aerodynamic Design of the High-Lift-Wing for a Megaliner Aircraft, Aerosp. Sci. Technol. 7 (2) (2003) 107–119.

[10]J. Tao, X.Y. Wang, G. Sun, Stall Characteristics Analyses and Stall Lift Robustness Inverse Design for High-Lift Devices of a Wide-Body Commercial Aircraft, Aerosp. Sci. Technol. 111 (2021) 106570.

[11]Ji Q, Zhang Y, Chen H, et al. Aerodynamic Optimization of a High-Lift System with Adaptive Dropped Hinge Flap[J]. Chinese Journal Of Aeronautics, 2022, 35 (11):191-208.

[12]Zhou W Y, Bai J Q, Qiao L, et al. A Study of Multi-Objective Aerodynamic Optimization Design for Variable Camber Airfoils and High Lift Devices[J]. Journal of Northwestern Polytechnical University, 2018, 36 (01): 83-90 (In Chinese).

[13]Ji Q, Zhang Y, Chen H, et al. Aerodynamic Optimization of a High-Lift System with Adaptive Dropped Hinge Flap [J]. Chinese Journal Of Aeronautics, 2022, 35 (11): 191-208.

[14]Tyan M, Park J-H, Kim S, et al. Design Optimization of Subsonic Airfoil and Slotted Flap Shape Using Multi-Fidelity Aerodynamic Analysis[C]. 21st Aiaa Computational Fluid Dynamics Conference, Aiaa Paper 2013-2704, 2013.

[15]Yang M, Yang W, Yang Zh G. Wind Tunnel Test of Ground Viscous Effect on Wing Aerodynamics[J]. Acta Aerodynamica Sinica, 2015,33(01):82-86 (in Chinese).

[16]Jia Q, Yang W, Yang Zh G. Numerical Analysis on Support Interference on Wing in Ground Effect Wind Tunnel Test[J]. Journal of Experiments in Fluid Mechanic, 2014,28(01):85-88 (in Chinese).

[17]Yang M, Yang W,Jia Q, et al.Experimental Study on Unsteady Flow of Wing-in-ground Effect at High Angle of Attack[J]. Advances in Aeronautical science and engineering, 2013,4(02):164-169 (in Chinese).

[18]HAN Z H, Kriging surrogate model and its application to design optimization :a review of recent progress[J]. Acta Aeronautica et Astronautica Sinica, 2016,37 (11):31973-225.

[19]HAN Z H, " SurroOpt: a Generic Surrogate-Based Optimization Code for Aerodynamic and Multidisciplinary Design," ICAS 2016, paper no. 2016_0281, Daejeon, Korea, 2016.

[20]Brenda M Kulfan. A Universal parametric geometry representation method- " CST " [C]. AIAA-2007-62,2007.

[21]Mckay M D, Beckman R J, Conover W J. Comparison of Three Methods for Selecting Values of Input Variables in the Analysis of Output from a Computer Code[J]. Technometrics, 1979, 21(2): 239-245.

[22]Jones, D R,: A Taxonomy of Global Optimization Methods Based on Response Surfaces[J]. Journal of Global Optimization, 2001, 21(4): 345-383.

[23]Han Z H, Zhang K S. Surrogate-based Optimization[M]. InTech Book,2012: 343-362.